A New Photonic Scheme for Generating 10-Fold Frequency Millimeter-Wave Signals Based on Four Parallel Polarization Modulators

DONGFEI WANG^{1,3*}, YANG MU¹, WEIPING ZHU¹, XIAOLING CHENG¹, LING XU³, YU WANG¹, JINJU TANG¹, CHENG YAO¹, XIAOKUN YANG^{1,2}, XIANGQING WANG^{1,2}

- ¹ School of Electronics and Information, Nanchang institute of technology, 330044, Jiangxi Province, China
- $^{\rm 2}$ School of Artificial Intelligence, Wuhan Technology and Business University, Wuhan 430065, China
- ³ Jiangxi Vocational and Technical College of Communications, Nanchang, 330013, Jiangxi Province, China
- *Corresponding author: wdfchina@126.com

Received: 01.09.2025

Abstract. The paper offers a detailed design and simulation analysis of a frequency 10-tupling millimeter-wave (mm-wave) signal generation method based on polarization modulation and optical sideband selection. In modern wireless communication systems, the need for high-frequency, high-capacity, and low-loss signal transmission has been continuously increasing. mm-wave technology, operating between 30 GHz and 300 GHz, provides a promising solution because of its wide bandwidth and high data rate potential. However, producing stable and pure mm-wave signals at high frequencies, especially at multiples of a base radio frequency, presents significant technical obstacles. Traditional direct frequency multiplication methods face issues like inefficient conversion, complex circuitry, and unwanted harmonic generation. To overcome these limitations, the proposed scheme uses polarization modulation and optical sideband filtering to achieve high-order frequency multiplication with better sideband suppression. The method involves a continuous wave laser, polarization controllers, polarization modulators (PolMs), electrical phase shifters, and a photodiode to produce a pure 10th-order mm-wave signal. By adjusting polarization angles, phase shifts, and modulation indices, unwanted harmonics are effectively removed. Simulation results show the accuracy and feasibility of the scheme, with the generated mm-wave signal having a high optical sideband suppression ratio of 63.6 dB and a radio frequency sideband suppression ratio of 56.089 dB. Although potential issues like bias-voltage drift, modulation-index inaccuracies, and the finite extinction ratios of PolMs may occur, the scheme provides a promising method for high-frequency mm-wave signal generation.

Keywords: millimeter-wave signal generation, polarization modulation technique, optical sideband selection, 10-fold frequency multiplication, radio frequency sideband suppression ratio, optical sideband suppression ratio **IIDC:** 535.8

DOI: 10.3116/16091833/Ukr.J.Phys.Opt.2026.01016

This work is licensed under the Creative Commons Attribution International License (CC BY 4.0).

1. Introduction

The rapid development of 5G/6G communication systems, satellite-ground integrated networks, and high-resolution radar systems has created an unprecedented need for millimeter-wave (mmwave) signals with frequencies above 100 GHz. These high-frequency signals are essential for enabling ultra-wideband data transmission, low-latency communication, and high-precision sensing. However, traditional electronic mm-wave generators, such as frequency multipliers and voltage-controlled oscillators, face fundamental limitations in bandwidth, power consumption, and phase noise when operating above 100 GHz. The electronic bottleneck becomes especially noticeable in scenarios requiring frequency multiplication factors greater than 8×, where parasitic effects and thermal noise impair signal quality [1-4].

Photonic techniques have emerged as a disruptive solution to overcome these challenges. By leveraging the high-frequency operation capability of optical components and the low-loss transmission properties of fiber-optic systems, photonic mm-wave generation enables seamless integration with radio-over-fiber (RoF) networks while achieving superior frequency tunability and phase noise performance. Among photonic approaches, frequency multiplication based on optical modulation has demonstrated significant potential. Traditional methods, such as Mach-Zehnder modulator (MZM)-based cascading and four-wave mixing (FWM) in highly nonlinear fiber, have achieved frequency multiplication factors up to 24-tupling [5]. Despite these advances, existing photonic frequency multiplication schemes often rely on complex configurations, such as multi-stage cascading or hybrid MZM-semiconductor optical amplifier systems, which introduce challenges in system stability, cost, and scalability. For example, the 24-tupling FWM-based method requires precise control of semiconductor optical amplifier gain and phase-matching conditions, whereas cascaded MZM schemes demand strict biasvoltage alignment to suppress unwanted sidebands [6]. Moreover, filterless architectures, which are essential for reducing system complexity, remain underexplored for high-order multiplication factors (e.g., ≥10-tupling) [7-8].

The generation of 10-tupling mm-wave signals using external modulators (phase modulators, MZM modulators, polarization modulators) remain relatively unexplored. A 10-tupling factor serves as a crucial intermediate step between lower-order (e.g., 8-tupling) and higher-order (e.g., 12-tupling, 16-tupling) multiplication schemes, balancing system complexity and frequency scalability. Ankita Rani [9] employed a dual-parallel configuration of MZMs to flexibly generate optical signals with multiple tupling factors (2, 4, 6, 8, 10, and 12) by controlling the bias point. However, this scheme depends on a MZM, and in actual experiments, the bias point drifts, necessitating additional complex control circuits. The scheme shows advantages at low frequencies, such as 2nd and 4th harmonics, with radio frequency sideband suppression ratio (RFSSR) reaching 36.34 dB. Yet at higher frequencies, such as the generation of 10th-tupled millimeter-wave signals, RFSSR is only 13.8 dB, making it challenging for communication applications. Jianhong Geng [10] proposed generating 10th-harmonic millimeter-wave signals using dual parallel MZMs and stimulated Brillouin scattering. In this scheme, the main modulator and the two sub-modulators of dual-parallel MZMs are both operated at the minimum transmission point to suppress the optical carrier and even sidebands. The modulation depth of the sub-modulators and the phase shift of the phase shifter are further adjusted to suppress the first- and seventh-order sidebands, leaving the third- and fifth-order sidebands. Then, the stimulated Brillouin scattering effect is used to filter out the third-order sidebands through Brillouin sideband filtering, retaining only the fifth-order sidebands. After sampling by a photodetector (PD), a 10th-tupled millimeterwave signal can be obtained. However, due to the complex structure and nonlinear effects, the RFSSR of the generated 10th-tupling-frequency millimeter-wave signal is only 24 dB.

Because polarization modulators lack bias points, they do not experience bias-point drift during millimeter-wave signal generation, thereby overcoming the problem of biaspoint drift in MZMs [11-13]. The paper proposes a new photonic scheme to generate frequency 10-tupling mm-wave signals using four parallel polarization modulators (PolMs). The proposed architecture exploits polarization multiplexing to selectively suppress the optical carrier and unwanted sidebands, enabling the generation of pure ±5th-order optical

sidebands. By optimizing the modulation index and phase differences between polarization states, the scheme achieves carrier-to-sideband suppression ratios exceeding 40 dB without the need for optical filters. Theoretical analysis and simulation results demonstrate that the proposed method can generate a 10-tupling mm-wave signal with a frequency tunability of up to 200 GHz, making it suitable for next-generation RoF systems and high-resolution radar applications. This work addresses the gap in high-order frequency multiplication by introducing a filterless, low-complexity PolM-based architecture. The proposed scheme not only advances the state of the art in photonic mm-wave generation but also provides a scalable platform for future research on sub-terahertz (Sub-THz) signal synthesis.

2. Principle of 10-tupling mm-wave signal generation

To achieve a 10-fold increase in the mm-wave frequency, a set of positive and negative 5th-order optical sidebands is needed to beat in the PD. However, obtaining pure \pm 5th-order optical sidebands is difficult because many unwanted harmonics also appear, such as 0th, \pm 2nd, \pm 3rd, \pm 4th, and \pm 6th order sidebands.

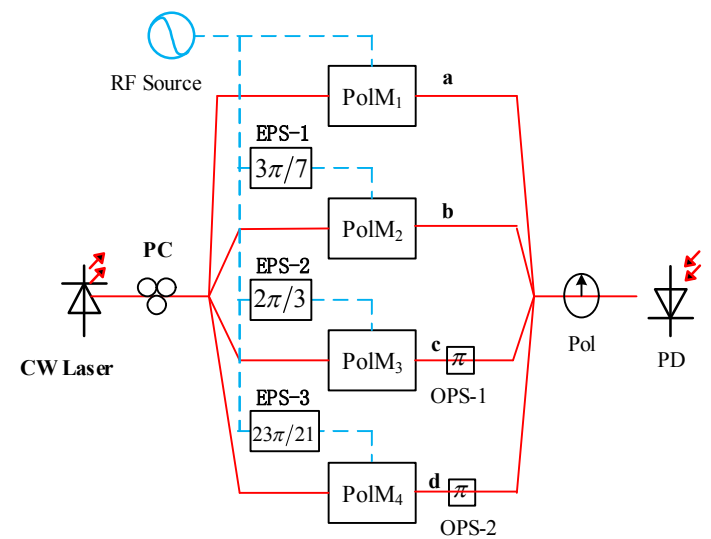


Fig. 1. Schematic diagram of the generation of a frequency 10-tupling mm-wave signal. RF: radio frequency; continuous wave; PC: polarization controller; PolM: polarization modulator; Pol: EPS: polarizer; electrical phase shifter; OPS: optical phase shifter; PC: polarization controller; PD: photodiode.

To obtain pure ± 5 th-order sidebands, the proposed scheme employs the following measurements to eliminate undesired harmonics. The continuous wave laser first radiates a light wave $E_{in} = E_c \exp(j\omega_c t)$, where E_c and ω_c are the amplitude and angular frequency of the optical carrier wave, respectively. The light wave output by the laser is first injected into the polarization controller (PC), with an azimuth angle of 45°. Then, it passes through a 1×4 beam splitter and is divided into four polarized light beams, which are respectively injected into the polarization modulators PolM₁-PolM₄ for modulation.

The output of a PolM can be described as:

$$\begin{pmatrix} E_{ix} \\ E_{iy} \end{pmatrix} = E_c \exp(j\omega_c t) \begin{bmatrix} \cos\theta_1 \exp(jm\cos(\omega_{RF}t + \phi_i)) \\ \sin\theta_1 \exp(-jm\cos(\omega_{RF}t + \phi_i)) \end{bmatrix}.$$
 (1)

In Eq. (1), $m = \pi V_{RF}/V_{\pi}$ is the modulation index of PolM, V_{π} is the half-wave voltage, V_{RF} is the amplitude of the driving voltage, θ_1 represents the azimuth angle of the polarization controller, ω_{RF} is the angular frequency of the driving RF signal, and ϕ_i is the phase offset of

the *i*-th PolM. At the adjusting the azimuth angle of the polarization controller to $\pi/4$, and adjusting the electrical phase shift of the phase shifter loaded on the PolM from the first channel to the fourth channel to 0, $3\pi/7$, $2\pi/3$, $23\pi/21$ respectively. The output of the first PolM (PolM₁) is:

$$\begin{pmatrix} E_{1x} \\ E_{1y} \end{pmatrix} = \frac{\sqrt{2}}{2} E_c \exp(j\omega_c t) \begin{bmatrix} \exp(jm\cos(\omega_{RF}t)) \\ \exp(-jm\cos(\omega_{RF}t)) \end{bmatrix}.$$
 (2)

The output of the second PolM (PolM₂) is:

The output of the third PolM (PolM₃) is:

The output of the fourth PolM (PolM₄) is:

$$\begin{pmatrix} E_{4x} \\ E_{4y} \end{pmatrix} = \frac{\sqrt{2}}{2} E_c \exp(j\omega_c t) \begin{bmatrix} \exp(jm\cos(\omega_{RF}t + 23\pi/21)) \\ \exp(-jm\cos(\omega_{RF}t + 23\pi/21)) \end{bmatrix}.$$
 (5)

If the signal output from the *i*-th modulator is injected into the Pol, the output signal is

$$E_{out-i}(t) = \begin{bmatrix} \cos \theta_2 & 0 \\ 0 & \sin \theta_2 \end{bmatrix} \begin{bmatrix} E_{ix} \\ E_{iy} \end{bmatrix} = E_{ix} \cos \theta_2 + E_{iy} \sin \theta_2.$$
 (6)

When controlling the polarization angle of Pol to $\theta_2 = -\pi/4$, the optical signal output by the *i*-th modulator can be described as:

$$E_{out-i}(t) = \begin{bmatrix} \cos \theta_2 & 0 \\ 0 & \sin \theta_2 \end{bmatrix} \begin{bmatrix} E_{ix} \\ E_{iy} \end{bmatrix} = \sqrt{2}/2 (E_{ix} - E_{iy})$$

$$= \frac{1}{2} E_c \exp(j\omega_c t) \left[\exp(jm \cos(\omega_{RF} t + \phi_i)) - \exp(-jm \cos(\omega_{RF} t + \phi_i)) \right].$$
(7)

Furthermore, the optical signals output by the third and fourth parallel polarization modulators undergo π -phase shifting before being coupled with the optical signals from the first and second parallel polarization modulators, and then injected into a polarizer with a polarization angle of $-\pi/4$. The output optical wave signal after Pol can be described as:

$$E_{out}(t) = \frac{1}{2}E_{c}\exp(j\omega_{c}t) \begin{cases} \left[\exp(jm\cos(\omega_{RF}t)) - \exp(-jm\cos(\omega_{RF}t))\right] \\ +\left[\exp(jm\cos(\omega_{RF}t+3\pi/7))\right] \\ -\exp(-jm\cos(\omega_{RF}t+2\pi/3)) \\ -\exp(-jm\cos(\omega_{RF}t+2\pi/3)) \right] \exp(j\pi) \end{cases}$$

$$+\left[\exp(jm\cos(\omega_{RF}t+2\pi/3))\right] \exp(j\pi)$$

$$+\left[\exp(jm\cos(\omega_{RF}t+23\pi/21))\right] \exp(j\pi)$$

$$= jE_{c}\exp(j\omega_{c}t) \begin{cases} \sin[m\cos(\omega_{RF}t)] + \sin[m\cos(\omega_{RF}t+3\pi/7)] \\ -\sin[m\cos(\omega_{RF}t+2\pi/3)] - \sin[m\cos(\omega_{RF}t+23\pi/21)] \end{cases}$$
(8)

By applying the Jacobi-Anger formula and expanding the above equation, we obtain:

$$E_{out}(t) = jE_{c} \exp(j\omega_{c}t) \begin{cases} \sin[m \cos(\omega_{RF}t)] + \sin[m \cos(\omega_{RF}t + 2\pi/7)] \\ -\sin[m \cos(\omega_{RF}t + 2\pi/3)] - \sin[m \cos(\omega_{RF}t + 23\pi/21)] \end{cases}$$

$$= jE_{c} \exp(j\omega_{c}t) \begin{cases} -2\sum_{n=1}^{\infty} (-1)^{n} J_{2n-1}(m) \cos[(2n-1)\omega_{RF}t_{1}] \\ -2\sum_{n=1}^{\infty} (-1)^{n} J_{2n-1}(m) \cos[(2n-1)(\omega_{RF}t + 2\pi/3)] \\ +2\sum_{n=1}^{\infty} (-1)^{n} J_{2n-1}(m) \cos[(2n-1)(\omega_{RF}t + 2\pi/3)] \\ +2\sum_{n=1}^{\infty} (-1)^{n} J_{2n-1}(m) \cos[(2n-1)(\omega_{RF}t + 23\pi/21)] \end{cases}$$

$$= -j2E_{c} \exp(j\omega_{c}t) \begin{cases} -J_{1}(m) \cos[\omega_{RF}t] + J_{3}(m) \cos[3\omega_{RF}t] - J_{5}(m) \cos[5\omega_{RF}t] \\ +J_{7}(m) \cos[\alpha_{RF}t] + m \end{cases} \begin{cases} -J_{1}(m) \cos[\omega_{RF}t + 2\pi/7] + J_{7}(m) \cos[3\omega_{RF}t + \pi + 2\pi/7] \\ -J_{5}(m) \cos[5\omega_{RF}t + 2\pi/7] + J_{7}(m) \cos[3\omega_{RF}t + 3\pi] + \cdots \end{cases} \end{cases}$$

$$= -j2E_{c} \exp(j\omega_{c}t) \begin{cases} -J_{1}(m) \cos[\omega_{RF}t + 2\pi/3] + J_{7}(m) \cos[3\omega_{RF}t + 3\pi + 2\pi/7] \\ -J_{5}(m) \cos[5\omega_{RF}t + 2\pi/3] + J_{7}(m) \cos[3\omega_{RF}t + 3\pi/7] \\ +J_{7}(m) \cos[\alpha_{RF}t + 2\pi/3] + \cos[\omega_{RF}t + 2\pi/3] + \cdots \end{cases}$$

$$= -j2E_{c} \exp(j\omega_{c}t) \begin{cases} -\cos[\omega_{RF}t] - \cos[\omega_{RF}t + 3\pi/7] \\ +\cos[\omega_{RF}t + 2\pi/3] + \cos[\omega_{RF}t + 2\pi/7] \end{cases}$$

$$= -j2E_{c} \exp(j\omega_{c}t) \end{cases}$$

$$= -j2E_{c} \exp(j\omega_{c}t) \begin{cases} -\cos[\delta\omega_{RF}t] + \cos[\delta\omega_{RF}t + 3\pi/7] \\ +\cos[\omega_{RF}t + 2\pi/3] + \cos[\omega_{RF}t + 2\pi/7] \end{cases}$$

$$= -j2E_{c} \exp(j\omega_{c}t) \end{cases}$$

$$= -j2E_{c} \exp(j\omega_{c}t) \begin{cases} -\cos[\delta\omega_{RF}t] + \cos[\delta\omega_{RF}t + 3\pi/7] \\ -\cos[\delta\omega_{RF}t] + \cos[\delta\omega_{RF}t + 3\pi/7] \end{cases}$$

$$= -j2E_{c} \exp(j\omega_{c}t) \rbrace$$

$$= -j2E_{c}$$

Due to the fact that

$$\begin{split} &\left\{\cos\left[3\omega_{RF}t\right] + \cos\left[3\omega_{RF}t + \pi + 2\pi/7\right] - \cos\left[3\omega_{RF}t + 2\pi\right] - \cos\left[3\omega_{RF}t + 3\pi + 2\pi/7\right]\right\} = 0\;,\\ &\left\{\cos\left[7\omega_{RF}t\right] + \cos\left[7\omega_{RF}t + 3\pi\right] - J_7(m)\cos\left[7\omega_{RF}t + 4\pi + 2\pi/3\right] - \cos\left[7\omega_{RF}t + 7\pi + 2\pi/3\right]\right\} = 0\;, \end{split}$$

the 3rd and 7th order optical sidebands tend to zero at the point at which the modulation index is equal to 3.83 (Fig. 2). Therefore, the output light wave can be represented as:

$$E_{out}(t) = -j2E_{c} \exp(j\omega_{c}t) \begin{cases} J_{1}(m) \begin{cases} -\cos[\omega_{RF}t] - \cos[\omega_{RF}t + 3\pi/7] \\ +\cos[\omega_{RF}t + 2\pi/3] + \cos[\omega_{RF}t + 23\pi/21] \end{cases} \\ +J_{5}(m) \begin{cases} -\cos[5\omega_{RF}t] + \cos[5\omega_{RF}t + 3\pi + \pi/3] \\ -\cos[5\omega_{RF}t + 2\pi + \pi/7] + \cos[5\omega_{RF}t + 5\pi + 10\pi/21] \end{cases} \end{cases}$$

$$0.6 \begin{cases} 0.2 \\ -0.4 \end{cases}$$

$$0.2 \end{cases}$$

$$0.4 \end{cases}$$

$$0.2 \end{cases}$$

$$0.4 \end{cases}$$

$$0.2 \end{cases}$$

$$0.4 \end{cases}$$

$$0.4 \end{cases}$$

$$0.5 \end{cases}$$

$$0.4 \end{cases}$$

$$0.5 \end{cases}$$

$$0.4 \end{cases}$$

$$0.6 \end{cases}$$

$$0.7 \end{cases}$$

$$0.7 \end{cases}$$

$$0.7 \end{cases}$$

$$0.7 \end{cases}$$

$$0.8 \end{cases}$$

$$0.9 \end{cases}$$

Fig. 2. Dependences of the first type Bessel function on the modulation index.

Fig. 2 shows the graph of the expansion of the first type Bessel function. It can be seen from the graph that when the modulation index is 3.83, the first-order function tends to zero. By adjusting the amplitude voltage of the RF drive signal, the modulation index can be controlled to make the modulation index m = 3.83. Then, the first-order optical sideband $J_1(m) \approx 0$, and the output light wave contains only the 5th-order optical sideband. Therefore, the final output light wave signal can be written as:

$$E_{out}(t) = -j2E_{c}\exp(j\omega_{c}t)J_{5}(m)\begin{cases} -\cos[5\omega_{RF}t] - \cos[5\omega_{RF}t + \pi/3] \\ -\cos[5\omega_{RF}t + \pi/7] - \cos[5\omega_{RF}t + 10\pi/21] \end{cases}$$

$$= jE_{c}\exp(j\omega_{c}t)J_{5}(m)\begin{cases} \exp(j5\omega_{RF}t)\left[1 + e^{j\pi/3} + e^{j\pi/7} + e^{j10\pi/21}\right] \\ +\exp(-j5\omega_{RF}t)\left[1 + e^{j\pi/3} + e^{j\pi/7} + e^{j10\pi/21}\right] \end{cases}$$

$$= jE_{c}\left[1 + e^{j\pi/3} + e^{j\pi/7} + e^{j10\pi/21}\right] \left\{\exp(j(\omega_{c} + 5\omega_{RF})t) + \exp(j(\omega_{c} - 5\omega_{RF})t)\right\}.$$
(11)

From Eq. (11), it can be seen that the output light wave only has a 5th order sideband, which can be further described as

$$E_{out}(t) = A \left[J_5(m) \exp(j\omega_c t + j5\omega_{RF} t) + J_5(m) \exp(j\omega_c t - j5\omega_{RF} t) \right], \tag{12}$$

where $A = jE_c[1 + e^{j\pi/3} + e^{j\pi/7} + e^{j10\pi/21}]$ is the amplitude of the output light wave.

Next, the light wave is injected into the PD for square law detection, resulting in a millimeter wave signal with a frequency ten times higher, which can be described as:

$$I_{PD}(t) \propto \Re \left| E_{out}(t) \right|^2$$

$$= \Re A^2 J_5^2(m) \cos(10\omega_{RF}t). \tag{13}$$

Here, \Re represents the responsivity of the PD.

3. Simulation results and analyses

To demonstrate the accuracy of the proposed mm-wave signal generation scheme, a simulation model was built on a simulation experiment platform based on the principle shown in Fig. 1. The parameter settings for the main components in the simulation are listed in Table 1.

Table 1. Main components parameters present in sin	mulation
---	----------

Tubic 21 1 ann componente parameters precent in simulation	
Parameters	Values
The center frequency of the CW laser	193.1 THz
CW laser linewidth	10 MHz
Power of CW laser	20 dBm
RF	10 GHz
Modulation index	3.83
Phase shift of EPS1	$3\pi/7$
Phase shift of EPS2	$2\pi/3$
Phase shift of EPS3	$23\pi/21$
Angle of PC	$\pi/4$
Angle of Pol	$-\pi/4$
Responsivity of PD	1 A/W
Dark current of PD	10 nA

A CW laser operating at 193.1 THz emits an optical wave. Adjust the angle of the PC to $\pi/4$ to generate linearly polarized light. Then, the linearly polarized light is split into four paths by a beam splitter. Use a sinusoidal signal with a frequency of 10 GHz as the input RF signal to drive four polarization modulators. The electrical phase offsets of PolMs numbered 1 to 4 loaded through EPS are $3\pi/7$, $2\pi/3$, and $23\pi/21$ rad, respectively. Finally, the signals are combined at an optical coupler and passed through a Pol to obtain the desired 10-fold multiplication of the frequency.

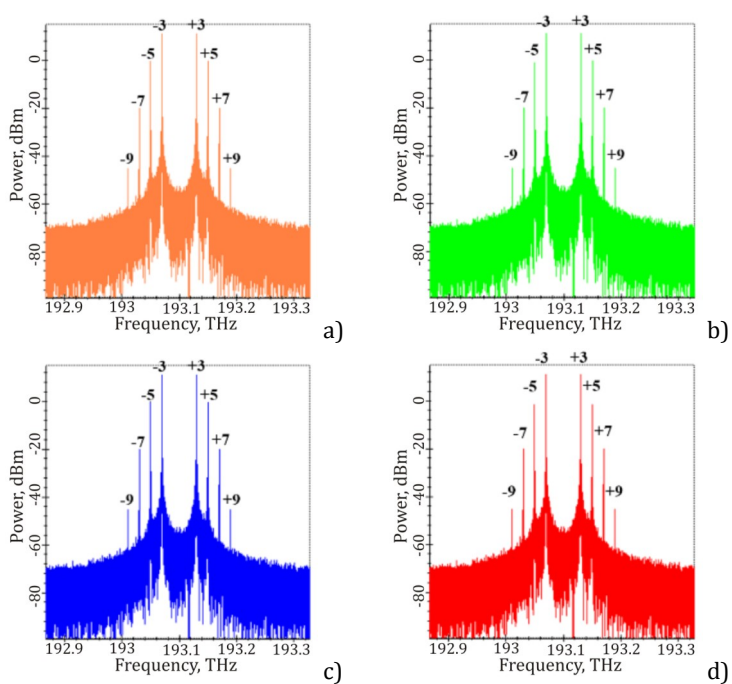


Fig. 3. The output optical spectrum diagrams obtained after (a) PolM1, (b) PolM2, (c) PolM3, and (d) PolM4.

The optical spectra obtained at different outputs are shown in Fig. 3. Examining each panel, such as (a), (b), (c), and (d), it is clear that there are ± 3 rd, ± 5 th, ± 7 th, and ± 9 th order optical sidebands. Because the power of the 9th order and higher is low, it can be ignored.

The optical spectrum is shown in Fig. 4. It can be seen that the optical wave consists of two main ±5th-order optical tones with a frequency spacing of 100 GHz, while other undesired sidebands, except for the 1st-order sidebands, are nearly suppressed. The fifth-order sidebands are 63.6 dB higher than the 1st-order sidebands, which is the optical sideband suppression ratio (OSSR).

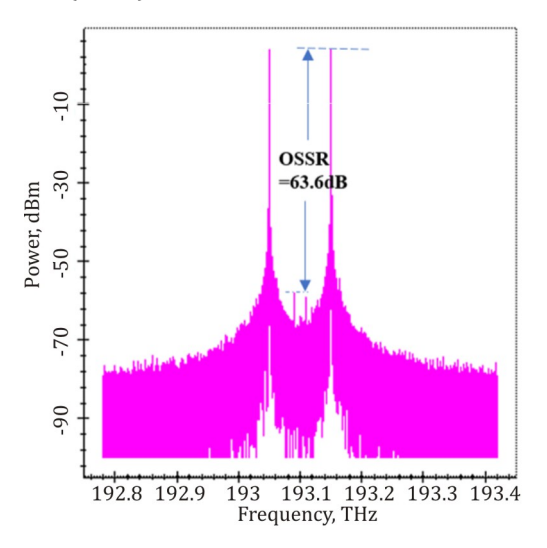


Fig. 4. The output optical spectrum diagram obtained after Pol.

The RF spectrum of the generated frequency 10-tupling optical mm-wave is shown in Fig. 5. We can see that the desired 100 GHz mm-wave signal is generated, and the spurious waves appear at 40 GHz and 60 GHz due to the presence of undesired ±1st-order sidebands. Nevertheless, the power of the 100 GHz mm-wave signal is 56.9 dB higher than that of the 40 GHz or 60 GHz mm-wave signal, which is the RFSSR.

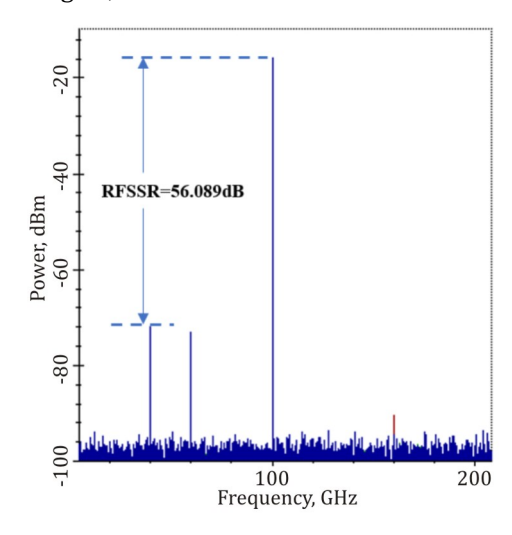
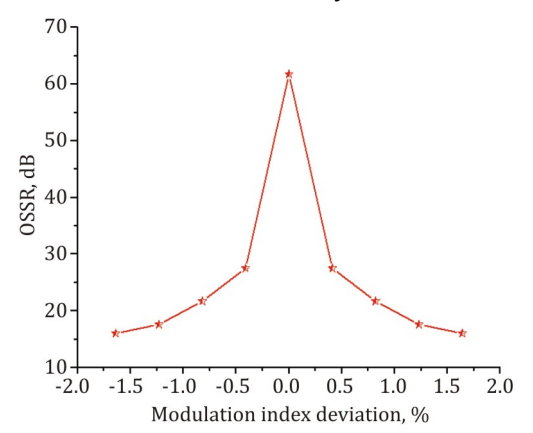


Fig. 5. The spectrum of the generated mm-wave signals with a 10-fold increase in frequency

The above theoretical principles and simulations assume that all controlled parameters are ideal values. However, in real experiments, achieving precise component operation is very challenging, which can impact the performance of the mm-wave signal. Several factors mainly contribute to the degradation of the 10-tupled signal. These include bias-voltage drift in the PolMs, an undesirable modulation index, and limited extinction ratios in the PolMs.

The modulation index, *m*, is used in this article as described above. Therefore, the modulation index is directly proportional to the voltage of the sine generator. When the RF source voltage deviates, the modulation index also deviates, leading to a deterioration in the quality of the generated millimeter-wave signal. The influence of modulation index on OSSR and RFSSR is shown in Fig. 6 and Fig. 7. From Fig. 6, it can be clearly seen that when the modulation index is 3.83, which means no deviation in the modulation index, OSSR and RFSSR reach their maximum values, making it the most suitable value for the modulation index. As the modulation index shifts, the values of OSSR and RFSSR decrease until the modulation index deviates by 1.5%, which is the maximum acceptable error range.



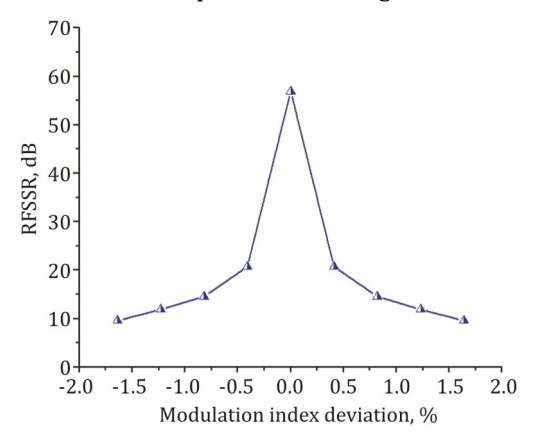


Fig. 6. The impact of modulation index deviation on OSSR.

Fig. 7. The impact of modulation index deviation on RFSSR.

4. Conclusion

In conclusion, this paper presents a frequency 10-fold mm-wave signal generation scheme based on polarization modulation and optical sideband selection, addressing the critical need for high-frequency, high-capacity wireless communication systems. The proposed method effectively removes unwanted harmonics by precisely controlling polarization angles, phase shifts, and modulation indices, resulting in a clean 10th-order mm-wave signal. Simulation results confirm the scheme's accuracy and feasibility, demonstrating high OSSR and RFSSR values. Overall, the introduced 10-fold mm-wave signal generation scheme represents an advancement in wireless communications.

Conflict of interest. The authors declare no conflict of interest. The authors declare that they have no known competing financial interests or personal relationships that could have influenced the work reported in this paper.

Data availability. The data can be obtained upon request from the authors.

Funding and acknowledgment. This work was supported by Jiangxi Provincial Natural Science Foundation (20232BAB212006, 2024AFB881), the first batch of general science and technology projects of Jiangxi Provincial Department of transportation in 2024 (2024YB031), Hubei Provincial Natural Science Foundation of China (2023AFB474), and Scientific Research Project of

the 14th Five-Year Plan of China Life Sciences Association(K1102024061014). The Education Reform and Development Project of "Integration of Industry and Education, School Enterprise Cooperation" of China Electronic Labor Society in 2024 (Cea12024136, Cea12024137). General Project of "Digital Empowerment Education" of China Adult Education Association in 2024 (2024-SJYB-007S).

References

- 1. Rani, A., & Kedia, D. (2024). Mathematical analysis of 24-tupled mm-wave generation using cascaded MZMs with polarization multiplexing for RoF transmission. *Optical and Quantum Electronics*, *56*(2), 193.
- 2. Kumar, A., Kedia, D., & Singla, S. (2025). 48-tuple mm wave generation scheme using remodulation with improved sideband suppression ratios. *Journal of Optics*, 1-15.
- Chen, L., Yu, Q., & Liu, J. (2023, June). Multifrequency Vector Mm-Wave Signal Generation with No Optical Filtering Based on One Dual-Arm MZM with Phase Factor Optimization. In *Photonics* (Vol. 10, No. 7, p. 747). MDPI.
- He, R., & Tousi, Y. (2022). A mm-wave signal generation and background phase alignment technique for scalable arrays. *IEEE Journal of Solid-State Circuits*, 58(2), 386-399.
- Xiaolei, L., Xing, S. (2023). Frequency 24-tupling ROF system based on cascaded DMZM. Journal of Quantum Optics, 29(1), 10702-1.
- Singh, S., Rani, A., & Kedia, D. (2023, February). Performance Analysis of 24-Tupled RoF System Based on Parallel MZMs and SOA. In *International Conference on Communication, Electronics and Digital Technology* (pp. 423-434). Singapore: Springer Nature Singapore.
- Asha, & Dahiya, S. (2023). Extinction ratio tolerant filterless millimeter wave generation using single parallel MZM. Optoelectronics Letters, 19(1), 14-19.
- 8. Al Wahaibi, Fawziya. (2021). *Millimeter wave generation techniques for future communication systems*. [Doctoral dissertation, Brunel University London]. PQDT Open. http://bura.brunel.ac.uk/handle/2438/24096
- Rani, A., & Kedia, D. (2022, February). Filterless millimeter-wave generation with tunable tupling factors using dual parallel-MZMs. In 2021 4th International conference on recent trends in computer science and technology (ICRTCST) (pp. 135-141). IEEE.
- Geng, H.-J & Hao, Sun & Zhao, Q.-S & Wang, Y. (2015). Frequency 10-tupling millimeter signal generation based on dual-parallel Mach-Zehnder modulator and stimulated Brillouin scattering. *Guangdianzi Jiguang/Journal of Optoelectronics Laser*, 26, 695-699.
- 11. Zhu, Z., Zhao, S., Li, X., & Li, Y. (2015, July). Microwave signal generation via frequency-sextupling using two cascaded polarization modulators without optical filter. In *2015 14th International Conference on Optical Communications and Networks (ICOCN)* (pp. 1-3). IEEE.
- 12. Abouelez, A. E. (2020). Photonic generation of millimeter-wave signal through frequency 12-tupling using two cascaded dual-parallel polarization modulators. *Optical and Quantum Electronics*, 52(3), 166.
- 13. Esakki Muthu, K., & Sivanantha Raja, A. (2018). Millimeter wave generation through frequency 12-tupling using DP-polarization modulators. *Optical and Quantum Electronics*, 50(5), 227.

Wang, D., Mu, Y., Zhu W., Cheng X., Xu L., Wang ,Y., Tang, J., Yao, C., Yang, X., Wang, X. (2026). A New Photonic Scheme for Generating 10-Fold Frequency Millimeter-Wave Signals Based on Four Parallel Polarization Modulators. *Ukrainian Journal of Physical Optics*, *27*(1), 01016 – 01026. doi: 10.3116/16091833/Ukr.J.Phys.Opt.2026.01026

Анотація. У цій роботі представлено детальний аналіз проєктування та результати моделювання схеми генерації сигналу міліметрового діапазону (мм-хвиль) з десятикратним множенням частоти, що ґрунтується на поляризаційній модуляції та виборі оптичних бічних смуг. У сучасних системах бездротового зв'язку спостерігається стале зростання попиту на високочастотну, високопропускну та низьковтратну передачу сигналів. Технологія мм-хвиль, яка функціонує у діапазоні 30–300 ГГц, розглядається як перспективне рішення завдяки широкій смузі пропускання та високій швидкості передачі даних. Водночас генерація стабільних та спектрально чистих мм-хвильових сигналів на високих частотах, зокрема на кратних гармоніках

базової радіочастоти, супроводжується значними технічними викликами. Традиційні методи прямого множення частоти характеризуються низькою ефективністю перетворення, складною схемотехнікою та утворенням небажаних гармонік. Для подолання цих обмежень у запропонованій схемі використано поляризаційну модуляцію та оптичну фільтрацію бічних смуг, що забезпечує високопорядкове множення частоти з покращеним придушенням побічних компонент. Розроблений метод передбачає застосування лазера з безперервним випромінюванням, контролерів поляризації, поляризаційних модуляторів, електричних фазозсувачів та фотодіода для формування чистого сигналу мм-хвилі десятого порядку. Шляхом оптимізації кутів поляризації, фазових зсувів та індексів модуляції досягається ефективне придушення небажаних гармонік. Результати моделювання підтверджують точність і практичну доцільність запропонованої схеми, при цьому згенерований сигнал міліметрового діапазону характеризується високим коефіцієнтом придушення оптичних бічних смуг на рівні 60,04 дБ та коефіцієнтом придушення радіочастотних бічних смуг 56,9 дБ. Попри потенційні фактори деградації, такі як дрейф напруги зміщення, неточності індексу модуляції та скінченні коефіцієнти загасання поляризаційних модуляторів, запропонована схема може розглядатися як перспективний підхід до генерації високочастотних сигналів міліметрового діапазону.

Ключові слова: генерація сигналів міліметрового діапазону, метод поляризаційної модуляції, вибір оптичної бічної смуги, 10-кратне множення частоти, коефіцієнт придушення бічної смуги радіочастот, коефіцієнт придушення оптичної бічної смуги